Journal of The Electrochemical Society, **147** (3) 1038-1045 (2000)
S0013-4651(99)08-021-0 CCC: $7.00

Faceting and Roughening Transitions on Copper Single Crystals in Acid Sulfate Plating Baths with Chloride

Q. Wu and D. Barkey*,z

Department of Chemical Engineering, University of New Hampshire, Durham, New Hampshire 03824, USA

Copper single-crystal surfaces were imaged by atomic force microscopy during copper deposition in acid sulfate solution with and without chloride. The appearance of singular facets depends on chloride concentration and on applied potential. The roughening and faceting transitions observed as potential was varied, and the stabilization of facets and terrace edges by chloride are analyzed in thermodynamic terms.

Manuscript received August 6, 1999.

Fabrication of copper structures smaller than 1 μm brings electrodeposition into a regime where the capillary potential is significant. Adsorbed additives can be expected to modify surface excess thermodynamic functions, and this may open one avenue for control of plating processes on small scales. While a number of theoretical and experimental investigations have focused on the role of surface excess free energy in morphology development, they have all proceeded from the assumption that it is isotropic.[1-7] However, its dependence on orientation may influence or control the growth form of crystals, and this dependence provides a link between the atomic-scale configuration of the surface and the macrosopic topography.[8-12]

The atoms on the surface of a copper crystal immersed in a plating bath approach an equilibrium configuration by galvanic action and by surface diffusion. On the macroscopic level, the crystal may be faceted at equilibrium, or it may be rounded, with a topography smoothed out by a nearly isotropic surface tension.[8,9] Corresponding to these macrotopographies are distinct microscopic configurations, the singular surface and the microscopically rough surface.[10] Facets give way to smoothly rounded features as the temperature is raised above the local roughening threshold.[11,12]

When the roughening transition was identified by Burton *et al*., its importance for the kinetics of crystal growth was recognized immediately.[10] Rough surfaces may grow by uniform attachment, while singular surfaces require creation of new layers by nucleation or emerging dislocations. More recently, scaling analysis has been applied to copper electrodeposition to obtain information on growth mechanisms and surface processes and their relation to surface structure.[13-17] The choice of models in this approach depends in part on the microscopic form of the surface. Some continuum models cannot reproduce faceted surfaces, even at equilibrium, because they do not include a lattice potential.[18] Even if the lattice potential is inserted into the models, its effect is eliminated at finite rates of growth. Another category of models has been used to examine singular surfaces, and they have shown that a kinetic barrier to transfer of adatoms from one terrace to another generates mounds bounded by vicinal faces.[19] This instability has been demonstrated for molecular beam epitaxy on Cu(100). [20] Hence, the surface type, singular or rough, must be considered in the choice of growth models.

At ambient temperature in vacuum, the equilibrium shape of copper is faceted, and even viscinal faces roughen only at elevated temperatures. Cu(110) has been shown to remain singular at least to 900 K, [21] and Cu(100) and Cu(111) to at least 770 K. [22] Using helium scattering, Villain *et al*.[23] found a roughening temperature T_r of 431 K for Cu(113), 356 K for Cu(115), and 315 K for Cu(117), while Fabre *et al*.[24] found T_r = 380 K for Cu(115). Measurements by X-ray scattering,[25] low-energy electron diffraction (LEED),[26] and He scattering[27] all find transition temperatures well above the range of plating processes. Hoogeman *et al*.[28] have reported direct observation of a roughening transition at 465 K on Ag(115) by scanning tunneling microscopy (STM), but we are not aware of any such measurements for copper.

While facets should appear on copper in vacuum, they are not always observed in sulfate solution. At the same time, they can be produced easily if chloride is added to the solution. These observations suggest that immersion in solution lowers the roughening temperature of copper surfaces by adsorption or by inclusion of contaminants,[26,29] and that the singular surfaces are restored by addition of chloride. There is evidence that the Cu(100) face is reversibly stabilized by chloride, and Vogt *et al*. have identified this stabilization as a thermodynamic effect based on microscopic evidence.[30-32] This microscopic organization of the surface by chloride may account for kinetic anisotropies and macroscopic pattern formation observed in copper electrodeposition from chloride solutons.[33,34]

We propose a thermodynamic interpretation of roughening and faceting transitions on copper surfaces in plating solutions which contain chloride. We have pursued this interpretation experimentally by observation of faceting and roughening on the submicrometer scale on copper single crystals. In the section that follows, relevant portions of the theory of equilibrium roughness and its relation to macroscopic faceting are presented. We consider how adsorbed chloride may stabilize the Cu(100) surface at equilibrium and relate this mechanism to simple models of thermal roughening. Atomic force microscopy (AFM) experiments on copper plating on Cu(100), Cu(111), and Cu(110) electrodes are then described and related to the theory.

Theory

Equilibrium between a copper crystal and an electrolyte solution containing the metal ion fixes the electrochemical potential μ of the metal, defined as the partial derivative of the total Gibbs free energy *G* of the solid phase with respect to the number of mole s *n* of metal at constant pressure and temperature

$$\mu = \frac{\partial G}{\partial n}\Big|_{p,T} \quad [1]$$

$$= \frac{\partial G_o}{\partial n}\Big|_{p,T} + \frac{\partial G_s}{\partial n}\Big|_{p,T} \quad [2]$$

Subscript o refers to the bulk phase and subscript s to the surface. The first term is the chemical potential of the bulk metal μ_o. The second term is obtained by integration of σ, the surface excess free energy per unit area, over the metal-solution interface

$$\mu = \mu_o + \frac{\partial}{\partial n}\int_S \sigma ds$$

Because the chemical potential of the metal has a single value, the second term can be expressed as a local constraint on the curvature κ.[8,9] For a two-dimensional crystal

* Electrochemical Society Active Member.
z E-mail: dpb@alberti.unh.edu

S0013-4651(99)08-021-0 CCC: $7.00

$$\mu = \mu_o + \kappa\nu\left(\sigma + \frac{\partial^2\sigma}{\partial\theta^2}\right) \quad [3]$$

$$= \mu_o + \kappa\nu\Psi \quad [4]$$

where ν is the molar volume and θ the local surface orientation. The sum of σ and its second derivative with respect to orientation is the surface stiffness Ψ.

According to Eq. 4, the electrochemical potential of a macroscopic or planar electrode, for which κ is either small or zero, is independent of surface orientation because addition or removal of material changes only the quantity of metal in the bulk and not the surface shape or area. For sufficiently small crystals or surface features, the curvature is appreciable, and the equilibrium potential is shifted from the bulk value by a capillary potential represented by the second term on the right side of Eq. 4.

To obtain the equilibrium shape, Eq. 4 is written in terms of surface orientation θ and a position coordinate l defined as distance along the surface

$$\kappa = -\frac{\partial\theta}{\partial l} = \frac{\mu - \mu_o}{\nu\Psi} \quad [5]$$

Along close-packed orientations at low temperature, the surface stiffness approaches infinity, and the curvature approaches zero, forming facets. Along these singular orientations, a negative curvature (convex) produces a negative capillary potential, and the protrusion retreats to form a flat interface. A positive curvature (concave) produces a positive capillary potential, and the surface advances to form a flat interface. For orientations with finite positive Ψ, Eq. 5 can be satisfied by a smooth convex or planar surface. Orientations with negative stiffness are unstable and do not appear in the equilibrium shape. For finite shapes, these directions form sharp corners, whereas planar surfaces of unstable orientation decompose to a hill-and-valley structure.[35] Similar remarks apply to terrace edges. An excess free energy per unit length may be defined, and from its dependence on orientation, the edge stiffness can be determined. Faceted terrace edges should be observed when the edge stiffness is infinite.

The stability and equilibrium curvature of a given orientation are functions of Ψ and not of σ alone. To produce infinite stiffness and facets, adsorption must be narrowly focused on a particular orientation, as for instance by a regular overlayer commensurate with the substrate at that orientation. The formation of such ordered overlayers has been documented for chloride on the Cu(100) [36-40] and Cu(111) [36,41,42] surfaces.

When the temperature exceeds the roughening threshold for a given surface, its stiffness is reduced, and it no longer appears as a facet in the equilibrium shape. On the microscopic level, this transition corresponds to a shift from the low-entropy, low-energy singular surface toward the high entropy surface populated by islands and adatoms.[26-28] While plating takes place below the vacuum roughening temperature, the energetics of the metal/solution interface are complicated by interactions that are coupled with the surface structure.[43,44] One possible result is chemical roughening by specific and nonspecific interactions at the interface[43] or by inclusion of contaminants in the metal matrix.[26,29] To illustrate how adsorbates may affect the energetics of the interface, we consider three simplified models: a solid-on-solid model,[10,45] an island-edge model,[46] and a terrace-ledge-kink model.[22]

In the solid-on-solid model, the energy penalty for placement of an adatom on the surface is added to the product of the temperature and the configurational entropy of the randomly distributed adatoms, and this expression for the surface excess free energy is minimized. The transition to a rough surface is gradual and occurs at approximately[10,45]

$$kT_r = \frac{L_o}{2}\frac{\eta_1}{\nu} \quad [6]$$

L_o is the binding energy of an atom in the bulk, η_1 the number of nearest neighbors in the same layer, and ν the number of nearest neighbors in the bulk.

In the island model, a partition function based on the energy of edge formation is computed. The edge-free energy vanishes, and islands of all sizes proliferate at temperatures above[46]

$$kT_r = \frac{J}{\ln\eta_1} \quad [7]$$

J is a coupling constant that gives the energy cost of a step change in the surface height.

Roughening of a viscinal surface may occur by proliferation of kinks at a temperature given implicitly by a terrace-ledge-kink model with step-step interactions[22]

$$kT_r = \frac{W_n}{2}\exp\left(\frac{W_o}{kT_r}\right) \quad [8]$$

W_n is an energy of interaction between steps, and W_o is the energy of kink formation.

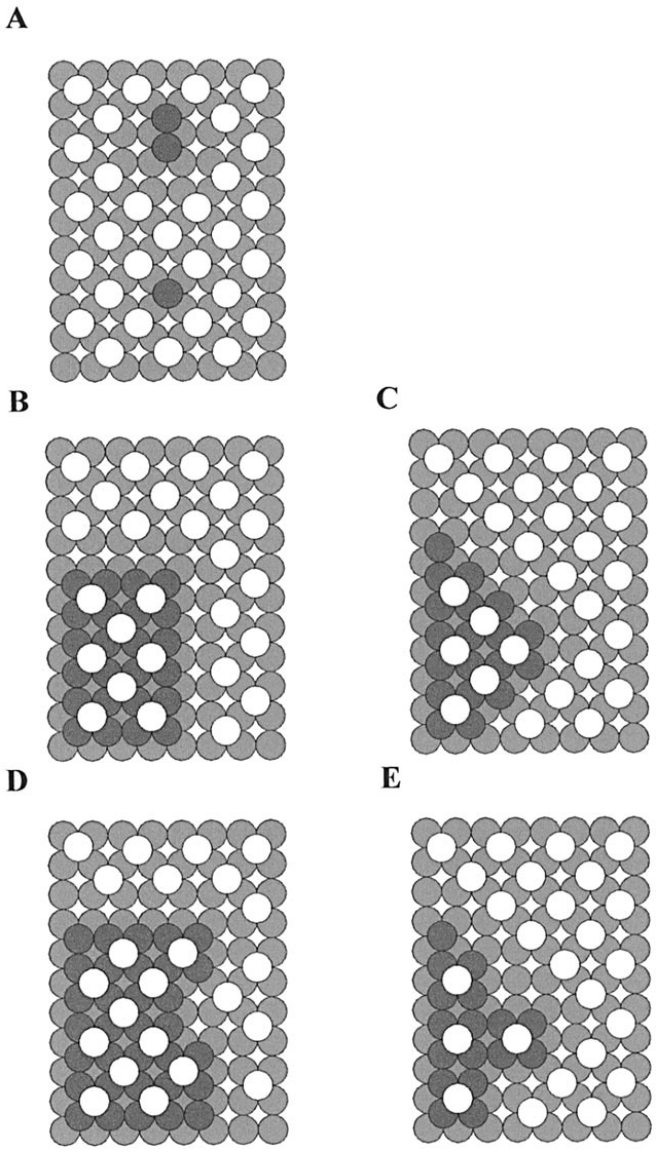

Figure 1. Schematic of Cu(100) surface with a $\sqrt{2} \times \sqrt{2}$ chlorine overlayer. The lower copper layer is shown in light gray, copper adatoms in dark gray, and chlorine in white. (A) adatoms; (B) terrace edge, (110) direction; (C) terrace edge, (100) direction; (D) kinks on the (110) edge; (E) kinks on the (100) edge.

S0013-4651(99)08-021-0 CCC: $7.00

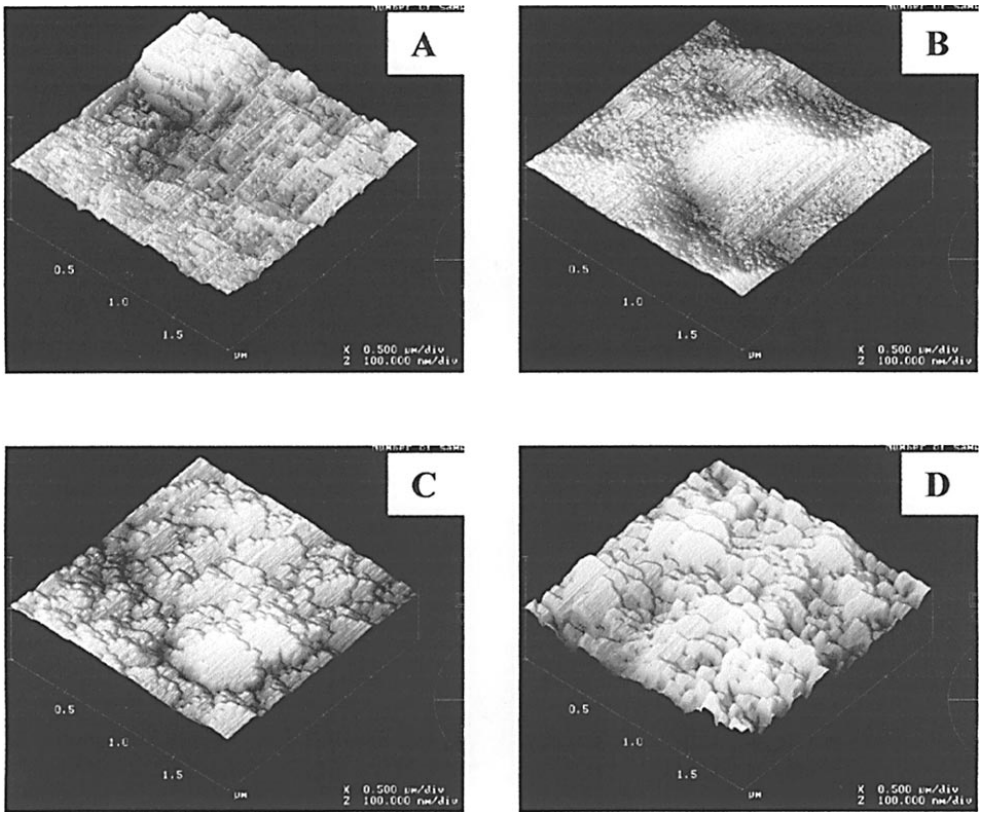

Figure 2. AFM images of Cu(100) in high-purity 0.01 M $CuSO_4$/1.0 M H_2SO_4. (A) −20, (B) −100, (C) −300, and (D) −400 mV.

According to these models, the roughening temperature will be reduced by immersion in solution if adsorption occurs preferentially at high-coordination sites. Such adsorption reduces the energy penalty L_o, J_o, or W_o for formation of adatoms, steps, or kinks by replacing metal-metal bonds with metal-adsorbate interactions. Conversely, the roughening temperature would be raised and faceting restored, if adsorption were to increase L_o, J_o, or W_o. This is the case for the $\sqrt{2} \times \sqrt{2}$ chlorine overlayer on the Cu(100) surface as shown in Fig. 1. The key assumption is that a chlorine atom may occupy the fourfold Cu hollow site only if the four adjacent hollow sites are

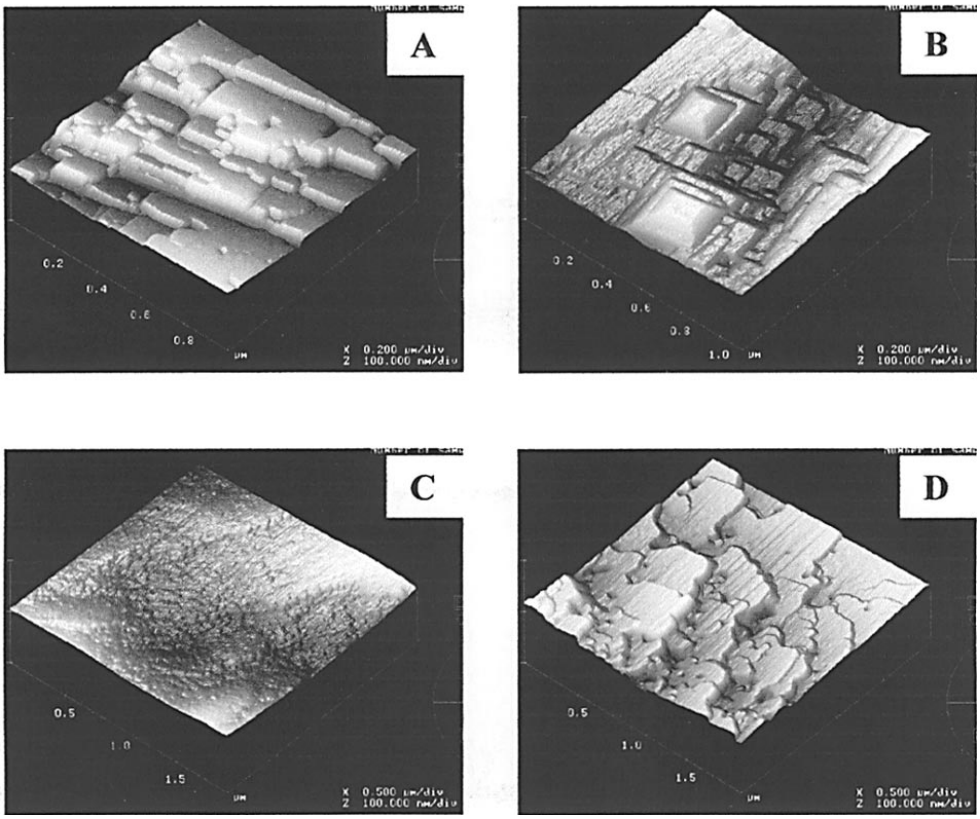

Figure 3. AFM images of Cu(100) in reagent 0.01 M $CuSO_4$/1.0 M H_2SO_4. (A) −20, (B) −100, (C) −200, and (D) −500 mV.

S0013-4651(99)08-021-0 CCC: $7.00

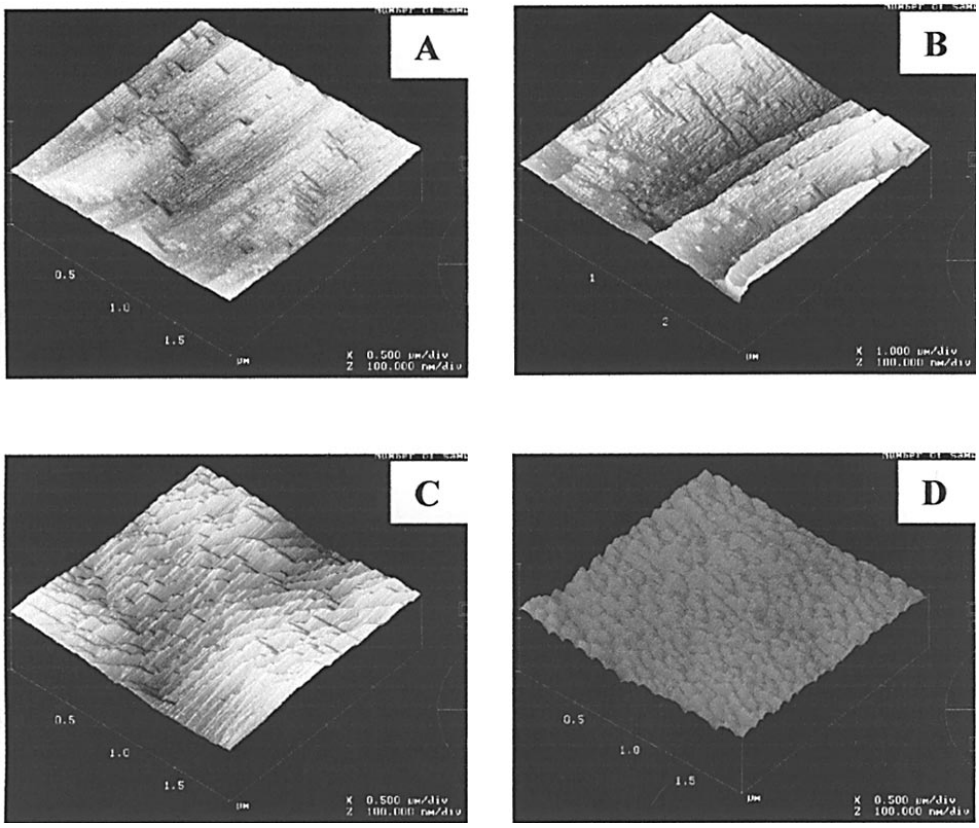

Figure 4. AFM images of Cu(100) in 0.01 M $CuSO_4$/1.0 M H_2SO_4/0.1 mM HCl. (A) −20, (B) −200, (C) −300, and (D) −500 mV.

empty. Figure 1a shows that addition of an adatom expels one chlorine atom while addition of a dimer expels four. The situation for formation of steps is shown in Fig. 1b and 1c. Vogt *et al.*[30] show this type of step arrangement as well as a second type in which chlorine atoms occupy positions at the edge where two adjacent fourfold sites are occupied by copper. Figure 1b shows that formation of a step along the (110) direction requires expulsion of chlorine from the surface because the adlayer rows on either side of the step are further apart than rows on the same level. Figure 1c shows the same effect for a step faceted along the (100) direction. Expulsion of the extra

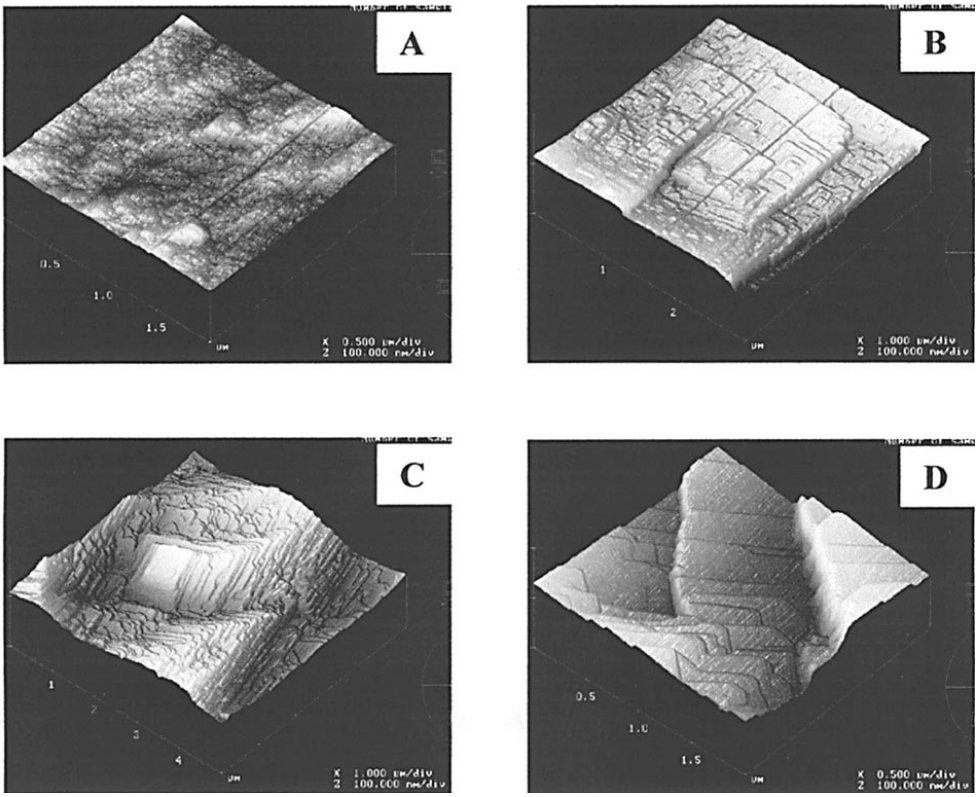

Figure 5. AFM images of Cu(100) in 0.01 M $CuSO_4$/1.0 M H_2SO_4/2.0 mM HCl. (A) −20, (B) −200, (C) −300, and (D) −500 mV.

S0013-4651(99)08-021-0 CCC: $7.00

chlorine atoms imposes an additional energy cost to adatom or step formation by effectively increasing the number of broken bonds, and it raises T_r.

The stability of terrace edges depends on the energetics of kink formation. Figure 1d shows formation of kinks on an edge oriented in the (110) direction. Formation of the kink pair expels a chlorine atom from the upper terrace, but creates a space for it on the lower terrace. Hence there is a no net expulsion of chlorine, and no extra energy cost for kink formation. As a result, this edge direction should be rough and not appear at equilibrium. Formation of a kink on an edge oriented in the (100) direction, however, does require expulsion of chlorine. As shown in Fig. 1e, no space on the lower terrace is created for the atom expelled from the upper terrace. Kink formation on this edge requires additional energy for removal of chlorine. Therefore, it should be stiff and appear in the equilibrium form. The stabilization of (100) terrace edges has been noted by prevous investigators, who observed that this corresponds to the close-packed direction of the overlayer.[30-32] We are advancing a different interpretation. The close-packed direction of the adlayer should be controlling if the energetics of the surface are dominated by chlorine-chlorine interactions. In the model advanced here, the energetics are dominated by the copper-chlorine interaction.

Experimental

Deposits were formed in dilute cupric sulfate to avoid rapid attack of the substrate by cupric ion. The basic solution was 0.01 M $CuSO_4$/1.0 M H_2SO_4. 0.1 mM or 2.0 mM chloride as HCl was added to two of the solutions. Two solutions without added chloride were prepared, one with reagent grade materials and another with Aesar Puratronic cupric sulfate and sulfuric acid. All of the solutions were made with demineralized water which was doubly distilled and passed through a Nanopure II filtration system. Copper single-crystal disks of orientations (100), (110), and (111) were obtained from Monocrystals Incorporated. They were polished with 0.05 μm alumina on an irrigated wheel and then electropolished in orthophosphoric acid. After polishing, the samples were rinsed sequentially in 10% nitric acid, 10% sulfuric acid, and water.

The surfaces were imaged with a Digital Instruments Nanoscope E AFM in both deflection and height mode. A standard AFM fluid cell with gold-coated spring clip, silicon nitride tips, and a 14 μm

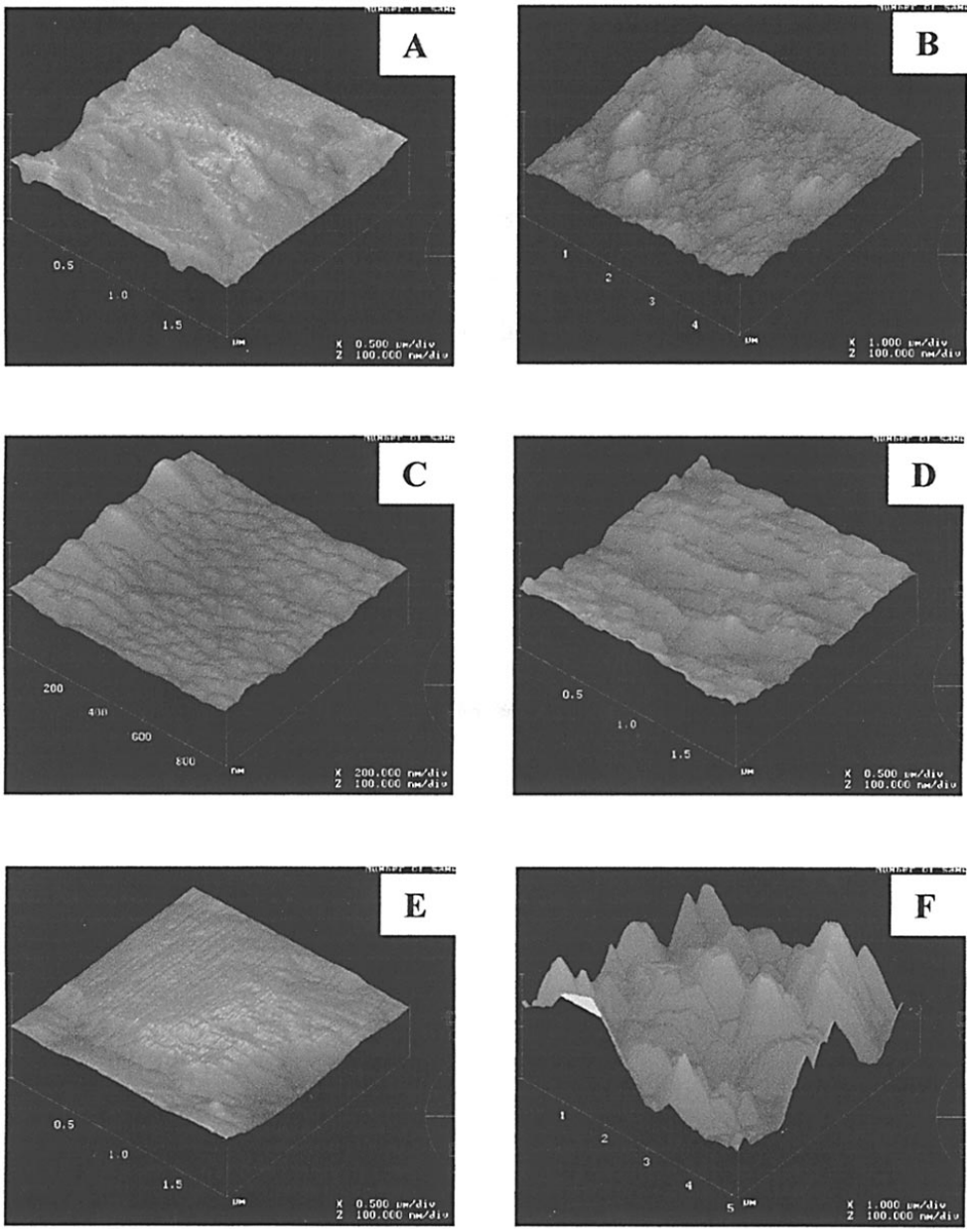

Figure 6. AFM images of Cu(110) in high-purity 0.01 M $CuSO_4$/1.0 M H_2SO_4 at (A) −100, (B) −300, and (C) −400 mV, and reagent 0.01 M $CuSO_4$/1.0 M H_2SO_4 at (D) −10, (E) −100, and (F) −200 mV.

S0013-4651(99)08-021-0 CCC: $7.00

scanner were used. The counter electrode and $Hg/HgSO_4$ reference electrode were placed in separate external reservoirs connected to the cell through the filling ports with polytetrafluorene-ethyl (PTFE) tubing. A constant potential was applied to the working electrode with an EG&G PAR model 362 potentiostat. The open-circuit potentials varied between −410 and −430 mV *vs.* the reference electrode. All potentials are reported *vs.* open circuit in the following sections. These potentials include ohmic loss within the cell as well as surface and concentration polarization. While the deposition process is necessarily removed from equilibrium, the currents in our experiments never exceeded 300 $\mu A/cm^2$. Other processes, such as adsorption and double-layer charging are relatively fast and are assumed to be at equilibrium. The surfaces reached a steady configuration at a given potential within 10 min, and the configurations could be reproduced by switching from one applied potential to another and back.

Results and Discussion

The purpose of the experiments was to distinguish between the singular and rough microstructures by identifying the corresponding faceted or isotropic features on the micrometer scale. Facets are indicated by flat regions, possibly containing distinct steps, and bounded by straight edges along regular and reproducible directions. By isotropic features, we mean rounded protrusions of random orientation lacking distinct steps. In high-purity chloride-free solution (Fig. 2) at a low overpotential of 20 mV, the main surface features produced on the Cu(100) surface were squares with edges facing the (100) direction. The height of the step edges was 2 to 5 nm. At 100-300 mV, the deposit did not produce a square geometry. Instead, the main features were rough nodules on which steps could not be distinguished and whose edges showed no preferred orientation. At 400-500 mV, faceted regions of the (100) orientation reappeared. Hence, the surfaces were weakly faceted at the highest and lowest overpotentials examined, and isotropic at intermediate overpotentials. At 600 mV, we observed isotropically rough surfaces on all orientations and in all four solutions, and the appearance of the surfaces was similar in every case. These surfaces were kinetically or diffusively roughened and are not considered further.

In reagent solution (Fig. 3), deposits on the (100) surface formed in the range from 20 to 100 mV were strongly anisotropic. The main features were truncated rectangular pyramids with edges parallel to the (100) direction. From 200 to 300 mV, isotropic edges and step heights of 2 to 5 nm were produced. At 500 mV, the layers were flat with edges along both the (100) and (110) directions and step heights greater than 20 monolayers. In 0.1 mM HCl (Fig. 4), truncated pyramids were produced at 200 to 300 mV. These grew by successive nucleation of layers with step heights of 2 to 5 nm. The edges were oriented in the (100) direction. In 2 mM HCl (Fig. 5), layer growth was observed at overpotentials greater than 150 mV, and at 300 mV, spiral growth with steps of a few nanometers appeared. In solutions with added chloride faceting is much sharper than in high-purity solution, and reagent solution produces faceting as well. The latter observation is probably the result of chloride present as a contaminant in reagent chemicals, which is known to influence the electrochemical behavior of copper.[47]

On the Cu(110) surface in high-purity solution (Fig. 6a-c), deposits showed little relation to the substrate orientation, although some anisotropy was visible at 400 mV. In reagent solution (Fig. 6d-f), ridges formed along the (100) direction at 10 mV. At 100 mV, the surface was nearly isotropic. At 200 to 300 mV, the surface was covered by truncated tetragonal pyramids with edges at an angle of 45° with the (100) direction. In 0.1 mM HCl (Fig. 7a-c), ridges of nearly uniform size extended along the (100) direction and were interrupted by (111) planes. In 2 mM HCl (Fig. 7d-f), the ridges were bounded by facets on the (210) and (111) planes. This is similar to the shape of depressions observed by Markovac after dissolution in sulfate solution.[48] The (110) surface decomposes into a faceted hill-and-valley structure when chloride is present.

On Cu(111) (Fig. 8), deposition at 100 mV produced a rough surface in high-purity solution. In reagent solution at the same potential, some terraces with hexagonal symmetry were visible. In 0.1 mM Cl and 2.0 mM Cl^-, the surface was covered by monoatomic terraces strongly faceted along the 112 direction. At this potential, hexagonal pits a few monolayers in depth interupted the terraces. The pits disappeared at higher overpotential, leaving only the

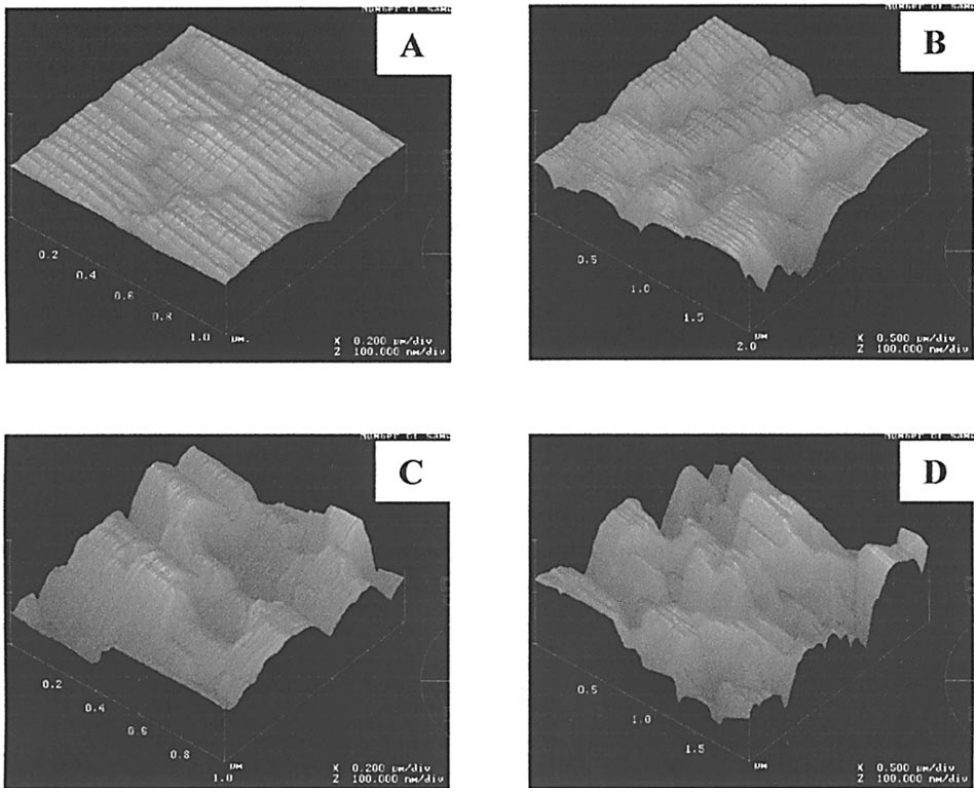

Figure 7. AFM images of Cu(110) in 0.01 M $CuSO_4$/1.0 M H_2SO_4/0.1 mM HCl at (A) −100 and (B) −200 mV, and 0.01 M $CuSO_4$/1.0 M H_2SO_4/2.0 mM HCl at (C) −100 and (D) −200 mV.

S0013-4651(99)08-021-0 CCC: $7.00

monoatomic steps. The terraces define shallow pyramids centered on screw dislocations and bounded by vicinal faces. The pyramids are separated by boundaries at which massive step bunching occurs. In the presence of chloride, the (111) surface is singular, nucleation is inhibited and growth occurs by advance of spiral terraces centered on dislocations. As we have reported previously, chloride produces faceting of monoatomic spiral edges on Cu(111).[49]

Conclusion

Copper immersed in solution may undergo adsorbate-induced roughening/faceting transitions at ambient temperatures. The strength of faceting decreases with decreasing chloride content in $CuSO_4/H_2SO_4$ solution. Faceting is promoted by chloride when it is present at low concentration, even as a contaminant in reagent solution. The (110) surface in 2.0 mM solution evidently has a negative surface stiffness. During deposition, this orientation disappears and is replaced by facets along close-packed directions. The (100) and (111) surfaces in the same solution are singular and exhibit terraces with well-defined edges. It is proposed that the formation of an ordered chloride overlayer on the Cu(100) surface, and the resulting increase in surface stiffness, accounts for the singular character of this orientation. It is also proposed that the chloride overlayer, because of its particular commensurate structure, also stiffens (100) edges, but not (110) edges, on the Cu(100) surface. The increase in surface stiffness induced by chloride adsorption can also be expected to inhibit nucleation, since it raises the energy required to construct a nucleus of small radius.

The observation of an ambient temperature transition from singular to microscopically rough surfaces suggests a thermodynamic route to brightening. A macroscopically smooth, thermodynamically rough surface is bright, whereas a microfaceted surface is not. If brighteners are specifically adsorbed at high coordination sites, they

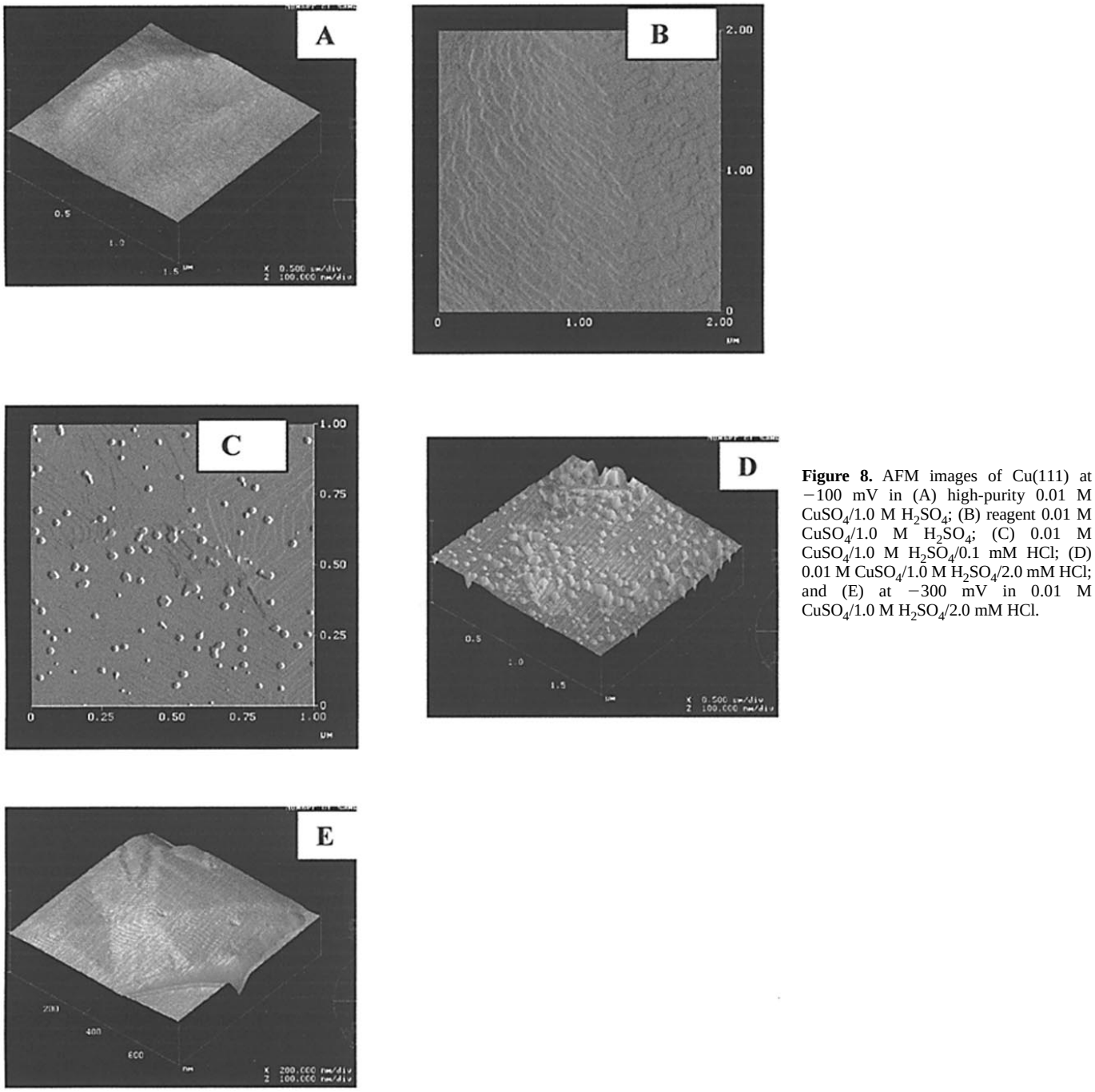

Figure 8. AFM images of Cu(111) at −100 mV in (A) high-purity 0.01 M $CuSO_4$/1.0 M H_2SO_4; (B) reagent 0.01 M $CuSO_4$/1.0 M H_2SO_4; (C) 0.01 M $CuSO_4$/1.0 M H_2SO_4/0.1 mM HCl; (D) 0.01 M $CuSO_4$/1.0 M H_2SO_4/2.0 mM HCl; and (E) at −300 mV in 0.01 M $CuSO_4$/1.0 M H_2SO_4/2.0 mM HCl.

S0013-4651(99)08-021-0 CCC: $7.00

will promote thermal roughening by reducing the energy of adatoms, steps, and kinks. The resulting microscopically rough surface will then grow by uniform advance, without the necessity of nucleation and step formation. Incorporation of the brightener or one of its components may also reduce surface stiffness and lead to a roughening transition.[26,29] At the same time, brighteners which operate by reducing the surface stiffness will promote nucleation.

Acknowledgments

This work was supported by the National Science Foundation under grant no. CTS-9622634 and CTS-9815067.

The University of New Hampshire assisted in meeting the publication costs of this article.

References

1. R. Aogaki, K. Kitazawa, Y. Kose, and K. Fueki, *Electrochim. Acta*, **25**, 965 (1980).
2. D. P. Barkey, R. H. Muller, and C. W. Tobias, *J. Electrochem. Soc.*, **136**, 2199 (1989).
3. D. P. Barkey, R. H. Muller, and C. W. Tobias, *J. Electrochem. Soc.*, **136**, 2207 (1989).
4. C. P. Chen and J. Jorne, *J. Electrochem. Soc.*, **138**, 3305 (1991).
5. M. D. Pritzer and T. Z. Fahidy, *Electrochim. Acta*, **37**, 103 (1992).
6. L-G. Sundstrom and F. H. Bark, *Electrochim. Acta*, **40**, 599 (1995).
7. J. Elezgaray, C. Leger, and F. Argoul, *J. Electrochem. Soc.*, **145**, 2016 (1998).
8. C. Herring, *Phys. Rev.*, **82**, 87 (1951).
9. C. Herring, in *Structure and Properties of Solid Surfaces*, R. Gomer and C. S. Smith, Editors, University of Chicago Press, Chicago, IL (1953).
10. W. K. Burton, N. Cabrera, and F. C. Frank, *Trans. Roy. Soc. London, A*, **243**, 299 (1951).
11. J. C. Heyraud and J. J. Metois, *Surf. Sci.*, **128**, 334 (1983).
12. J. C. Heyraud and J. J. Metois, *J. Cryst. Growth*, **82**, 269 (1987).
13. G. L. M. K. S. Kahanda, X. Zou, R. Farrell, and P. Wong, *Phys. Rev. Lett.*, **68**, 3741 (1992).
14. H. Iwasaki and T. Yoshinobu, *Phys. Rev. B*, **48**, 8282 (1993).
15. H. Iwasaki, T. Yoshinobu, and H. Iwasaki, *Phys. Rev. Lett.*, **72**, 4025 (1994).
16. W. U. Schmidt, R. C. Alkire, and A. A. Gewirth, *J. Electrochem. Soc.*, **143**, 3122 (1996).
17. S. Mendez, G. Andreasen, P. Schilardi, M. Figueroa, L. Vasquez, R. C. Salvarezza, and A. J. Arvia, *Langmuir*, **14**, 2515 (1998).
18. A. L. Barabasi and H. E. Stanley, *Fractal Concepts in Surface Growth*, Cambridge University Press, Cambridge, U.K. (1995).
19. J. Villain, *J. Phys. I*, **1**, 19 (1991).
20. H. J. Ernst, F. Fabre, R. Folkerts, and J. Lapujulaude, *Phys. Rev. Lett.*, **72**, 112 (1994).
21. P. Zeppenfeld, K. Kern, R. David, and G. Comsa, *Phys. Rev. Lett.*, **62**, 63 (1989).
22. J. Lapujoulade, J. Perreau, and A. Kara, *Surf. Sci.*, **129**, 59 (1983).
23. J. Villain, D. R. Grempel, and J. Lapujoulade, *J. Phys. F*, **15**, 809 (1985).
24. F. Fabre, D. Gorse, J. Lapujoulade, and B. Salanon, *Europhys. Lett.*, **3**, 737 (1987).
25. K. S. Liang, E. B. Sirota, K. L. D'Amico, G. J. Hughes, and S. K. Sinha, *Phys. Rev. Lett.*, **59**, 2447 (1987).
26. J. Wollschlager, E. Z. Luo, and M. Henzler, *Phys. Rev. B*, **44**, 44 (1991).
27. H. J. Ernst, R. Folkerts, and L. Schwenger, *Phys. Rev. B*, **52**, 52 (1995).
28. M. S. Hoogeman, M. A. J. Klik, D. C. Schlosser, L. Kuipers, and J. W. M. Frenken, *Phys. Rev. Lett.*, **82**, 1728 (1999).
29. B. E. Sundquist, *Acta. Metall.*, **12**, 585 (1964).
30. M. R. Vogt, A. Lachenwitzer, O. M. Magnussen, and R. J. Behm, *Surf. Sci.*, **399**, 49 (1998).
31. M. R. Vogt, F. A. Moller, C. M. Schilz, O. M. Magnussen, and R. J. Behm, *Surf. Sci.*, **367**, L33 (1996).
32. T. P. Moffat, *Mater. Res. Soc. Proc.*, **451**, 75 (1997).
33. D. Barkey, F. Oberholtzer, and Q. Wu, *Phys. Rev. Lett.*, **75**, 2980 (1995).
34. F. Oberholtzer, D. Barkey, and Q. Wu, *Phys. Rev. E*, **57**, 6955 (1998).
35. W. W. Mullins, *Philos. Mag.*, **6**, 1313 (1961).
36. J. L. Stickney, C. B. Ehlers, and B. W. Gregory, *Langmuir*, **4**, 1368 (1988).
37. I. Villegas, C. B. Ehlers, and J. L. Stickney, *J. Electrochem. Soc.*, **137**, 3143 (1990).
38. C. B. Ehlers and J. L. Stickney, *Surf. Sci.*, **239**, 85 (1990).
39. C. B. Ehlers, I. Villegas, and J. L. Stickney, *J. Electroanal. Chem.*, **284**, 403 (1990).
40. J. L. Stickney, I. Villegas, and C. B. Ehlers, *J. Am. Chem. Soc.*, **111**, 6473 (1989).
41. D. W. Suggs and A. J. Bard, *J. Am. Chem. Soc.*, **116**, 10725 (1994).
42. J. L. Stickney and C. B. Ehlers, *J. Vac. Sci. Technol. A*, **7**, 1801 (1988).
43. F. Silva, M. J. Sottomayor, and A. Martins, *J. Chem. Soc., Faraday Trans.*, **92**, 3693 (1996).
44. D. D. Sneddon, D. M. Sabel, and A. A. Gewirth, *J. Electrochem. Soc.*, **142**, 3027 (1995).
45. D. P. Woodruff, *The Solid-Liquid Interface*, Cambridge University Press, Cambridge, U.K. (1973).
46. A. Zangwill, *Physics at Surfaces*, Cambridge University Press, Cambridge, U.K. (1988).
47. Z. Nagy, J. P. Blandeau, N. C. Hung, L. A. Curtiss, and D. J. Zurawski, *J. Electrochem. Soc.*, **142**, L87 (1995).
48. V. Markovac, *J. Electrochem. Soc.*, **119**, 1461 (1972).
49. Q. Wu and D. Barkey, *J. Electrochem. Soc.*, **144**, L261 (1997).